Cross-Linked Long-Pitch Actin Dimer Forms Stoichiometric Complexes with Gelsolin Segment 1 and/or Deoxyribonuclease I That Nonproductively Interact with Myosin Subfragment 1[†]

Hans Georg Mannherz,*[,‡,§] Edda Ballweber,[‡,||] György Hegyi,[⊥] and Roger S. Goody[§]

Department of Anatomy and Embryology, Ruhr-University, Bochum, Germany, Department of Biochemistry, Eötvös Loránd University, Budapest, Hungary, Max-Planck-Institute of Molecular Physiology, Dortmund, Germany, and Institute for Physiological Chemistry, Ruhr-University, Bochum, Germany

Received March 10, 2008; Revised Manuscript Received July 1, 2008

ABSTRACT: Actin dimer cross-linked along the long pitch of the F-actin helix by *N*-(4-azido)-2-nitrophenyl (ANP) was purified by gel filtration. Purified dimers were found to polymerize on increasing the ionic strength, although at reduced rate and extent in comparison with native actin. Purified actin dimer interacts with the actin-binding proteins (ABPs) deoxyribonuclease I (DNase I) and gelsolin segment-1 (G1) as analyzed by gel filtration and native gel electrophoresis. Complex formation of the actin dimer with these ABPs inhibits its ability to polymerize. The interaction with rabbit skeletal muscle myosin subfragment 1 (S1) was analyzed for polymerized actin dimer and dimer complexed with gelsolin segment 1 or DNase I by measurement of the actin-stimulated myosin S1-ATPase and gel filtration. The data obtained indicate binding of subfragment 1 to actin dimer, albeit with considerably lower affinity than to F-actin. Polymerized actin dimer was able to stimulate the S1-ATPase activity to about 50% of the level of native F-actin. In contrast, the actin dimer complexed to DNase I or gelsolin segment 1 or to both proteins was unable to significantly stimulate the S1-ATPase. Similarly, G1:dimer complex at 20 μM stimulated the rate of release of subfragment 1 bound nucleotide (mant-ADP) only 1.6-fold in comparison to about 9-fold by native F-actin at a concentration of 0.5 μM. Using rapid kinetic techniques, a dissociation constant of 2.4×10^{-6} M for subfragment 1 binding to G1:dimer was determined in comparison to 3×10^{-8} M for native F-actin under identical conditions. Since the rate of association of subfragment 1 to G1:dimer was considerably lower than to native F-actin, we suspect that the ATP-hydrolysis by S1 was catalyzed before its association to the dimer. These data suggest an altered, nonproductive mode for the interaction of subfragment 1 with the isolated long-pitch actin dimer.

Beginning with its first isolation from muscle tissue by Straub (*1*) it has become abundantly clear that actin is one of the most ubiquitous proteins in nature. It exists in two forms, as monomeric or G-actin and filamentous or F-actin. In many nonmuscle cells the amount of G-actin is similar to that of polymerized actin and represents a reserve pool of actin sequestered by binding to particular actin-binding proteins, whereas F-actin is the physiologically active form, building the microfilaments in nonmuscle cells and the backbone of the thin filaments in muscle cells. In nonmuscle cells actin participates in a large number of diverse cellular motile events. For these processes to occur the intracellular microfilament system is constantly restructured by regulated interactions of actin with a large number of actin-binding proteins, among which the most relevant group is probably the myosin family. Together with myosin, actin is involved in force-generating processes during muscle contraction and cell migration. The motor protein myosin exists in two basic different forms: the family of the classical two-headed myosin present in muscle and most nonmuscle cells and the large group of single-headed myosins in nonmuscle cells. Myosins consist of a tail region of varying length associated with a variable set of light chains and a head region, which contains the actin-binding and ATPase sites. By limited proteolytic cleavage of, for instance, skeletal muscle myosin II or genetic engineering the head together with a variable part of the tail region can be obtained in isolated and soluble form.

The actin monomers are helically oriented within F-actin. Their helical orientation can be described by a one-start left-handed generic helix with an axial rise of about 55 Å and rotation of −166° or by a two-start right-handed helix with a pitch of about 380 Å, also termed the long-pitch helix. During recent years the atomic structures of actin in complex with different actin-binding proteins (*2–5*) and of the head regions of a number of myosins (*6, 7*) have been elucidated. However, high-resolution structural information about the actin−actin contacts within F-actin and the actin−myosin

[†] H.G.M. and E.B. were supported by a grant (SPP "motor proteins") from the Deutsche Forschungsgemeinschaft (Bonn, Germany).

* To whom correspondence should be addressed. Tel: +49-234-3224553. Fax: +49-234-3214474. E-mail: hans.g.mannherz@rub.de.

[‡] Department of Anatomy and Embryology, Ruhr-University.

[§] Max-Planck-Institute of Molecular Physiology and Institute for Physiological Chemistry, Ruhr-University.

[||] Present address: AEROPHARM GmbH, Francois-Mitterand-Allee, D-07407 Rudolstadt, Germany.

[⊥] Department of Biochemistry, Eötvös Loránd University.

10.1021/bi800410z CCC: $40.75
Published on Web 08/12/2008

interface is still lacking, although fiber diffraction analysis and model building resulted in a ca. 8 Å resolution map of the structure of F-actin (*8, 9*).

Actin monomers within F-actin can be cross-linked to generate chemically cross-linked dimers and higher molecular mass oligomers. Depending on the actin residues involved in the cross-linking reaction, dimers can be generated that stabilize different contact areas and orientations of monomers within F-actin. By use of the photoactive cross-linker *N*-(4-azido-2-nitrophenyl)putresceine (ANP),[1] cross-links can be generated between Gln-41 and Cys-374 of two adjacent actin monomers along the long-pitch helix (*10–12*). The polymerization properties of thus cross-linked F-actin and isolated actin dimer and oligomers were previously analyzed (*12*). The interface of adjacent actin monomers along the long-pitch helix is assumed to represent the binding region for many F-actin-binding proteins and in particular for myosin. Indeed, the elucidation of the three-dimensional structure of this dimer has recently verified that it represents a long-pitch dimer (*13*). As a minimal F-actin, this dimer would be ideally suited for functional and structural studies of the interaction of a number of binding proteins with F-actin. So far, the published analysis of the interaction of F-actin generated from ANP-cross-linked actin and isolated dimer suggested that they fully activate the Mg^{2+}-dependent subfragment 1 ATPase but did not fully support the actin-activated force generation by myosin as tested in an in vitro motility assay (*14, 15*).

Because of the attractiveness of the long-pitch dimer as an ideal binding partner for a large number of actin-binding proteins and myosin, we isolated the ANP-cross-linked dimer (AA) and analyzed its polymerization behavior and interaction with the actin-binding proteins DNase I and gelsolin segment 1 (G1) with the aim of inhibiting its ability to polymerize. We furthermore analyzed the ability of the complexes G1:AA and AA:DNase I to interact with the active head region of rabbit skeletal muscle myosin with light chain 1 (subfragment 1 = S1A1). Our results, however, indicate that the ANP-cross-linked dimer does not fully simulate the functions of F-actin, since it binds considerably more weakly to S1A1 and does not stimulate the Mg^{2+}-dependent ATPase of myosin subfragment 1.

MATERIALS AND METHODS

Materials. Sephacryl S300 and Sephadex G150 superfine were obtained from Pharmacia (Freiburg, Germany). The EnzCheck phosphate measuring kit was from Molecular Probes (supplied by MoBiTec, Göttingen, Germany). 3′-*O*-(*N*-Methylanthranidoyl)adenosine 5′-triphosphate (mant-ATP) was prepared as described (*16*). All other reagents were of analytical grade. Anti-actin antibody was purchased from Sigma (Munich, Germany), and the polyclonal anti-myosin subfragment 1 antibody had been generated in rabbits and described earlier (*17*). Protein microconcentrators with a cutoff of 30 kDa "centricon-30" were obtained from Amicon (Witten, Germany). Salmon sperm DNA was from Sigma (Munich, Germany); all other reagents were of analytical grade.

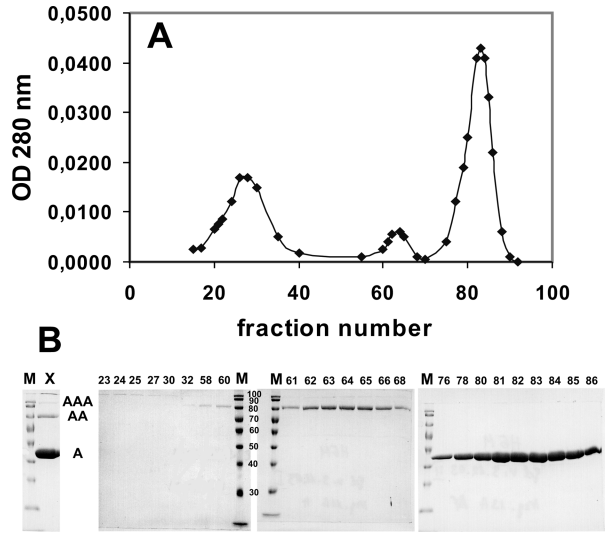

FIGURE 1: Purification of actin dimer over Sephadex G150 column. (A) gives elution profile; fraction size 3 mL. (B) gives SDS−PAGE analysis of fractions collected by 10% acrylamide gels. Fraction numbers are indicated over the gels. M gives prestained marker (M_r are indicated in kDA between first and second gel) and X the cross-linked actin preparation before column loading (A = monomeric, AA = dimeric, and AAA = trimeric actin).

Protein Preparations. Rabbit skeletal muscle actin was prepared from dried acetone powder (*18*). The purified G-actin was dialyzed against Hepes buffer (5 mM Hepes-OH, pH 7.5, 0.5 mM ATP, 0.2 mM $CaCl_2$, and 3 mM NaN_3) and cross-linked by ANP exactly as detailed in ref *12*. Bovine pancreatic DNase I was a commercial product from Paesel & Lorei (Frankfurt, Germany) and further purified by chromatography on hydroxylapatite (*19*). The N-terminal domain of cytoplasmic gelsolin (segment 1 = G1) was expressed in *Escherichia coli* and purified as described (*20*). Rabbit skeletal muscle myosin was isolated from rabbit psoas muscle as described in ref *18*, and chymotryptic subfragment 1 was prepared and separated into S1A1 and S1A2 isoforms (*21*). SDS−PAGE indicated that subfragment 1 containing the light chain A1 (S1A1) was almost 100% pure, but occasionally contained in addition a trace amount of the light chain A2. Pyrene-labeled actin (pyrenyl-actin) was prepared exactly as detailed by Koujama et al. (*22*).

Analytical Procedures. Protein concentrations were determined either by a colorimetric assay (*23*) or of actin by measuring the optical density at 290 nm (0.63 = 1 mg/mL) using a Beckman DU 640 spectrophotometer. SDS−PAGE was performed according to ref *24* and routinely performed to check the purity of prepared proteins. For native gel electrophoresis 7.5% polyacrylamide gels were used as described previously (*25*). Steady-state rates for the Mg^{2+}-dependent ATPase of S1A1 stimulated by F-actin or actin dimer were determined using the linked enzyme EnzCheck phosphate measuring assay at 37 °C as recommended by the manufacturer (see also legend to Figure 4). DNase I activity was determined by measuring the increase in absorbance at 260 nm of 50 μg/mL salmon sperm DNA (hyperchromicity test) (*19*) using a Beckman spectrophotometer DU 640. DNase I activity is expressed in Kunitz

[1] Abbreviations: AA, cross-linked actin dimer; ABP, actin-binding protein; ANP, *N*-(4-azido)-2-nitrophenyl; DNase I, deoxyribonuclease I (EC 3.1.21.1); G1, N-terminal segment 1 of gelsolin; MESG, 2-amino-6-mercapto-7-methylpurine riboside; PNP, purine nucleoside phosphorylase; S1A1, subfragment 1 with light chain A1.

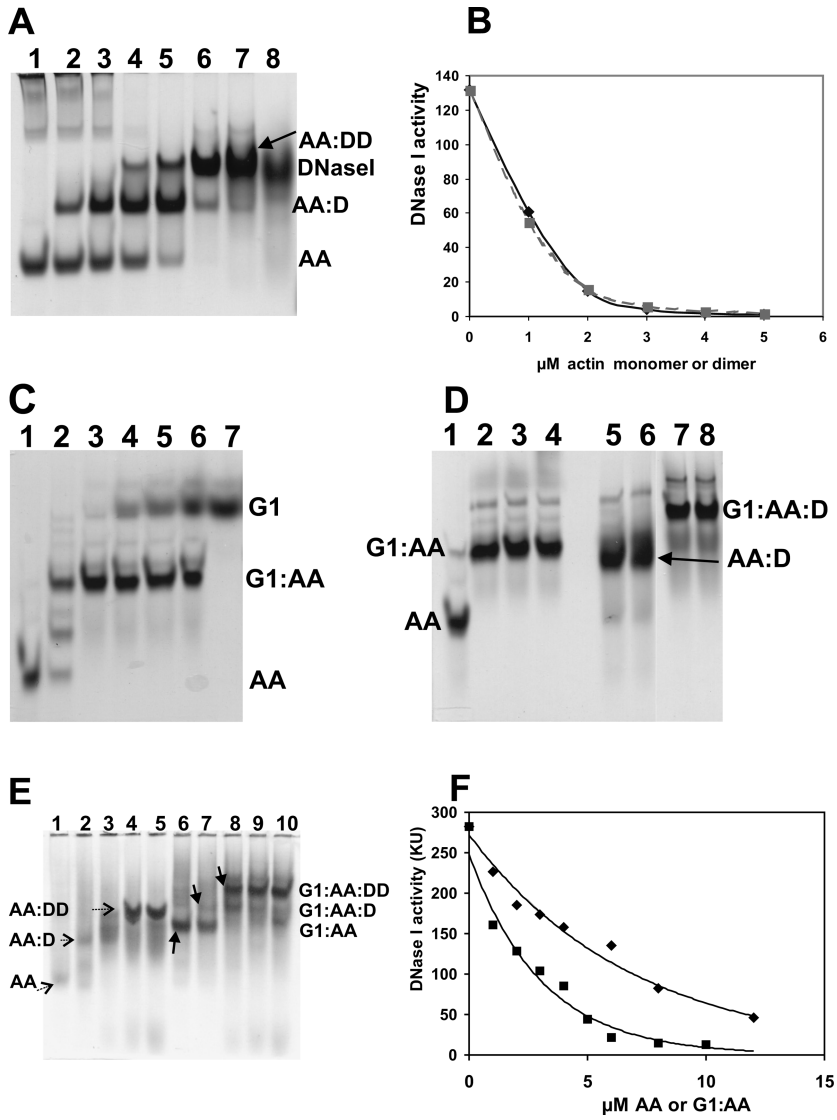

FIGURE 2: Interaction of actin dimer with gelsolin segment 1 (G1) and DNase I. (A) Native gel of actin dimer (4.8 μM final concentration, lane 1) mixed with increasing concentrations of DNase I (lane 2, plus 1.16 μM; lane 3, 2.32 μM; lane 4, 3.53 μM; lane 5, 4.66 μM; lane 6, 9.33 μM; lane 7, 18.66 μM DNase I). Lane 8 gives 18.66 μM DNase I on its own. (B) Inhibition of DNase I activity (DNase I set at 5 μM) by increasing concentrations of actin dimer (■) and monomeric actin (◆). Abscissa gives dimer or G-actin concentrations as monomer concentration. Ordinate gives DNase I activity in Kunitz units (KU; 1 KU = ΔOD_{260nm} of 0.001/min). (C) Native gel of actin dimer (4.8 μM final concentration, lane 1) mixed with increasing concentrations of G1 (lane 2, plus 2.9 μM; lane 3, 5.8 μM; lane 4, 8.7 μM; lane 5, 11.6 μM; lane 6, 14.5 μM G1). Lane 7 gives 14.5 μM G1 on its own. (D) Native gel to prove ternary complex formation between actin dimer, DNase I, and G1. Lane 1, actin dimer alone at 4.1 μM; lanes 2 and 3, plus 13.7 μM G1; lanes 5 and 6, plus 16.7 μM DNase I; lanes 7 and 8, plus 13.7 μM G1 and 16.7 μM DNase I. (E) Native gel of increasing DNase I concentrations added to dimer (lanes 1−5) and to G1:dimer complex (lanes 6−10). Mixtures applied to gel contained 5 μM actin dimer (on its own in lane 1) or G1:dimer complex (5 μM DNase I plus 7.5 μM G1 in lane 6) plus 1.66 μM (lanes 2 and 7), 5.0 μM (lanes 3 and 8), 7.5 μM (lanes 4 and 9), and 13.2 μM DNase I (lanes 5 and 10). Arrows with pointed arrow lines give actin dimer (AA), dimer:DNase I (AA:D), and dimer:2DNase I complex (AA:DD), respectively. The arrows in lanes 6−8 point to G1:dimer (G1:AA), G1:dimer:DNase I (G1:AA:D), and G1:dimer:2DNase I complex (G1:AA:DD), respectively. (F) Inhibition of DNase I (10 μM) activity by actin dimer (■) and G1:dimer complex (◆) added at increasing concentrations (given in dimer concentration = 2 actin subunits). Ordinate gives DNase I activity in Kunitz units (KU; 1 KU = ΔOD_{260nm} of 0.001/min).

units (KU). One KU corresponds to a change in optical density at 260 nm (ΔOD_{260nm}) of 0.001/min at 25 °C.

Measurement of Polymerization Kinetics. Actin polymerization was measured by the fluorescence increase of pyrene-labeled actin at wavelength settings at 365 and 385 nm for excitation and emission or by light scattering with wavelength settings at 315 and 318 nm for excitation and emission, respectively, using a Schimadzu RF 5001PC fluorometer.

Stopped-Flow Experiments. Stopped-flow experiments for transient kinetics were performed at 20 °C in 5 mM Hepes-OH, pH 7.4, 0.1 mM $CaCl_2$, 0.5 mM DTT, and 1 mM NaN_3 with an Applied Photophysics stopped-flow apparatus (Leatherhead, U.K.) using a 150 W Xe/Hg lamp. The appropriate wavelengths settings were set at 360 nm for excitation by use of a monochromator and at 395 nm for emission by an appropriate filter. All protein concentrations given refer to the concentrations after mixing into the stopped-flow observation cell holding ca. 50 μL reactant mixture.

Determination of Mant-ADP Dissociation from S1. Nucleotide displacement from subfragment 1 by actin was monitored using mant-ADP (3′-*O*-(*N*-methylanthranidoyl)-adenosine 5′-diphosphate). Purified S1A1 was incubated with

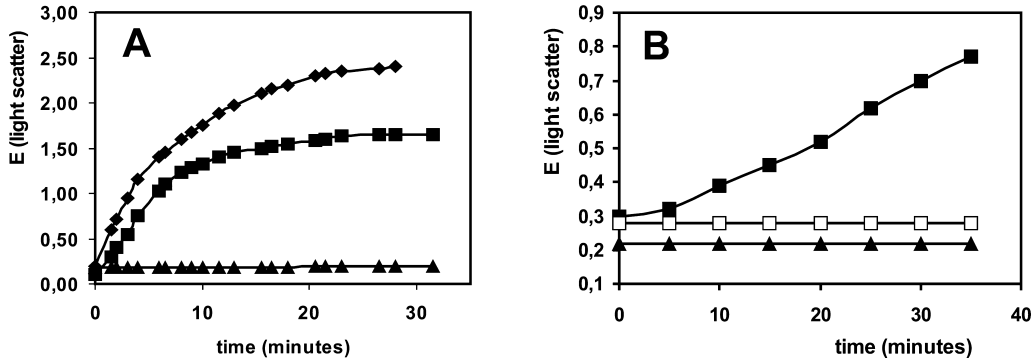

FIGURE 3: Rate of polymerization of native and dimeric actin. (A) Actin polymerization was initiated at time zero by addition of 0.1 M KCl and 2 mM $MgCl_2$: (◆) native actin (2 μM final concentration); (■) actin dimer (at 2 μM dimer concentration = 4 μM actin monomer concentration); and (▲) actin dimer (at 2 μM dimer concentration) complexed to DNase I, G1, or DNase I and G1 at equimolar dimer concentration. Polymerization was followed by light scattering as detailed in text. Ordinate gives intensity of scattered light (E) in arbitrary units. (B) Induction of polymerization by S1A1 (2.54 μM) in the absence of salt of (■) actin dimer (2 μM), (□) AA:DNase I, and (▲) G1:AA (both at 2 μM). Ordinate gives intensity of scattered light (E) in arbitrary units.

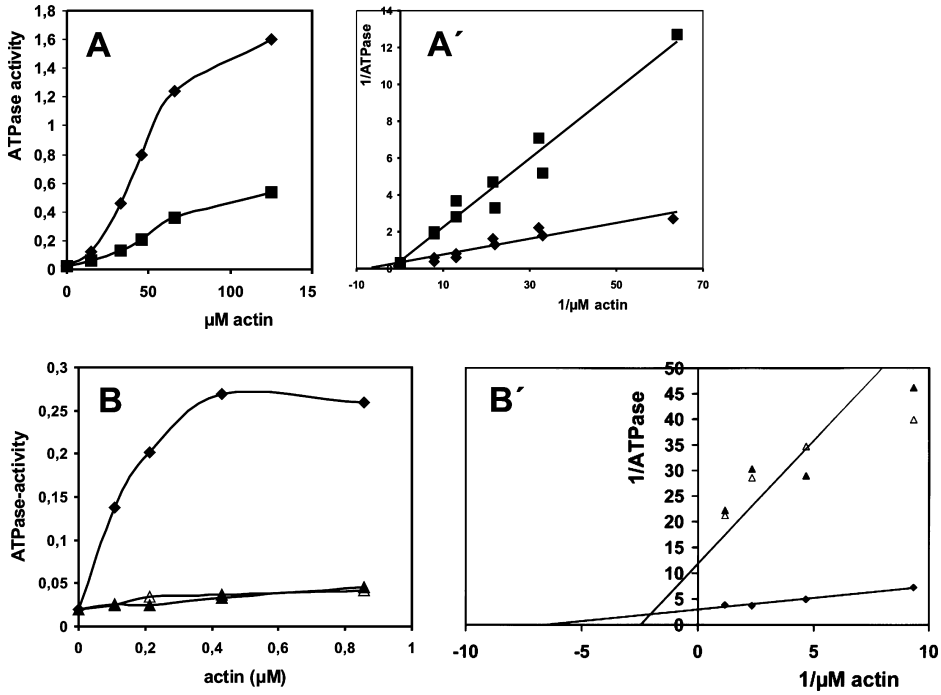

FIGURE 4: Stimulation of the Mg^{2+}-dependent myosin subfragment 1 ATPase. Native actin and purified dimer were polymerized by addition of 2 mM $MgCl_2$ for 1 h and subsequently added to the test solution composed of 5 mM Hepes-OH, pH 7.4, 0.1 mM $CaCl_2$, 0.5 mM NaN_3, 50 mM KCl, and 2 mM $MgCl_2$ supplemented with 4 mM MESG substrate and 0.5 unit of purine nucleoside phosphorylase (PNP) (EnzCheck, Molecular Probes) plus 1.27 μM S1A1 in a volume of 250 μL. The reaction was started by addition of 0.1 mM ATP, and after 5 min the actin samples were added to the concentrations indicated. The reaction was followed for 10−20 min at 360 nm in a Beckman DU640 spectrophotometer. (A) gives the ATPase stimulation by (◆) native F-actin and (■) polymerized actin dimer. (A′) gives the double-reciprocal representation of the data 1/v against 1/actin monomer concentration. (B) gives the ATPase stimulation by (◆) native F-actin, (△) G1:AA, and (▲) G1:AA:DNase I at the actin monomer concentrations indicated on the abscissa. (B′) gives the corresponding double-reciprocal representation.

either a stoichiometric amount of mant-ATP overnight at 4 °C in order to allow complete hydrolysis to mant-ADP (*18*) or with a 4-fold molar excess of mant-ADP. Binding of mant-nucleotide to S1 results in a fluorescence increase that can be monitored with wavelength settings of 356 and 445 nm for excitation and emission, respectively, or 290 nm for excitation when using fluorescence energy transfer (FRET) between subfragment 1 tryptophans and mant-ADP. After rapid mixing of F-actin or actin dimer complexed to G1 (G1:AA) with mant-ADP-S1A1 the release of mant-ADP was determined by its fluorescence decrease.

Determination of the Dissociation Constant of Subfragment 1 Actin Dimer Complex. Stopped-flow measurements to determine the rates of association and dissociation of S1A1 to F-actin were performed with pyrene-labeled F-actin (F-pyr-actin) generated by polymerization of an equimolar mixture of native and pyrene-labeled G-actin by addition of 2 mM $MgCl_2$ in Hepes buffer. The fluorescence decrease of F-pyrene-actin after subfragment 1 binding was followed after rapid mixing with wavelength settings of 360 and 395 nm for excitation and emission, respectively. For the determination of the affinity of S1A1 to G1:AA we employed a competition assay, in which subfragment 1 was mixed with a constant concentration of F-pyrene-actin containing increasing concentrations of G1:AA.

RESULTS

Isolation of Cross-Linked Actin Dimer. Rabbit skeletal muscle actin was cross-linked by ANP as described (*10, 11*) and in Materials and Methods and subsequently dialyzed against Hepes buffer plus 0.2 mM ATP for 3 days with frequent changes of the dialysis solution. SDS−PAGE analysis demonstrated that the cross-linked actin contained about 40% monomer and in addition dimeric, trimeric, and tetrameric cross-linked actins with decreasing concentration in this order (Figure 1B, lane X). After a clearing spin for 1 h at 100000*g* the actin solution was applied to a Sephadex G150 column (dimensions: 2.5 × 90 cm) and eluted with G buffer containing 0.2 mM ATP at a flow rate of 7 mL/h. A typical elution profile and a resulting SDS−PAGE analysis of the collected fractions (size 3 mL) are shown in Figure 1. The obtained dimer fractions were pooled and concentrated by centricon-30 (Amicon) to about 1−2 mg/mL.

Interaction of Actin Dimer with DNase I and Gelsolin Segment 1. First we analyzed the interaction of the purified actin dimer (AA) with the actin-binding proteins DNase I and gelsolin segment 1 (G1) by native gel electrophoresis. Addition of an equimolar concentration of DNase I resulted in a shift of the dimer to a new position of lower migratory ability (Figure 2A, lanes 1−4). When the DNase I concentration was further increased to a 2:1 ratio of DNase I with respect to the actin dimer concentration, a second shift occurred to a new position of further decreased mobility (Figure 2A, lanes 5−7), suggesting that both actin monomers of the dimer are able to bind DNase I. This assumption was tested by an analysis of the inhibitory ability of the dimer on DNase I activity. When titrating DNase I activity with increasing dimer concentration, we noted that at equimolar actin subunit to DNase I concentration its DNA degrading was inhibited to only about 50%, whereas full inhibition was obtained when the dimer concentration was that of DNase I, i.e., at double monomer concentration as verified by the comparison with native G-actin (Figure 2B). This result indicates that only one monomer of the actin dimer is able to inhibit the DNase I activity, although both appear to be able to bind DNase I. Indeed, it has been shown previously that under certain conditions binding of DNase I to monomeric actin does not necessarily lead to its inhibition (*26*).

Next we tested the binding of gelsolin segment 1 (G1) to actin dimer by native gel electrophoresis. Addition of increasing concentrations of G1 also resulted in a shift of the dimer to a new position of lower migratory ability (Figure 2C). This position was not altered even when the molar concentration of G1 exceeded that of the dimer by a factor of 5 (Figure 2C).

Using native gel electrophoresis, we also tested whether the dimer was able to simultaneously bind DNase I and G1. In the simultaneous presence of G1 and DNase I a further shift from the position of AA:DNase I was obtained, indicating the formation of a ternary complex between the actin dimer, G1, and DNase I (Figure 2D). Complex formation between actin dimer and G1 or DNase I was also verified by gel filtration on Sephacryl S200 (data not shown). Next we tested whether binding of G1 influenced the interaction of the dimer with DNase I. To this aim we compared the binding of DNase I to dimer and to G1:dimer complex by native gel electrophoresis. The data obtained indicated a higher affinity of the G1:dimer than dimer alone to DNase I, since the shift to the dimer:2DNase I complex occurred at lower DNase I concentration for the G1:dimer complex (Figure 2E). Similarly, G1:dimer inhibited DNase I more effectively than uncomplexed dimer. Indeed, 90% inhibition of DNase I was attained at half-equimolar dimer concentration, indicating that in the G1:dimer complex both actin subunits were not only able to bind DNase I but also able to inhibit DNase I (Figure 2F). In contrast, the stoichiometric 1:1 complex of unmodified G-actin with G1 did not exhibit any difference in DNase I inhibition in comparison to G-actin alone (data not shown).

Polymerization Behavior of Actin Dimer Alone and in Complex with G1 and/or DNase I. This was first investigated by light scattering. The dimer alone was found to polymerize, as suggested by the increase in light scattering after addition of 1−2 mM $MgCl_2$ or 0.1 M KCl or both, although at a lower rate and to a lower extent than unmodified G-actin (Figure 3A). After complexing the dimer with DNase I or G1 or both, dimer polymerization was completely prevented (Figure 3A), indicating that these actin-binding proteins inhibited dimer polymerization as in case of native G-actin whose polymerization is also completely inhibited by binding to DNase I (*19*) and the N-terminal segment G1 of gelsolin (*3*). Addition of myosin subfragment 1 (S1A1) to actin dimer induced its slow polymerization even in the absence of salt, whereas the inhibition of polymerization of G1:AA, AA:DNase I, or G1:AA:DNase I was maintained in the presence of S1A1 (Figure 3B). In the presence of salt, S1A1 induced a faster rate of polymerization of actin dimer, as also previously reported (*12*), but dimer complexed to DNase I, G1, or both remained polymerization resistant (data not shown).

Isolated Dimer Does Not Stimulate the Myosin Subfragment 1 ATPase. First we compared the ability of polymerized dimer and native F-actin to stimulate the Mg^{2+}-dependent S1A1 ATPase. Using the EnzCheck system to measure released phosphate, we found that polymerized purified actin dimer stimulated the S1-ATPase to a considerably lower extent than native F-actin (Figure 4A). A double-reciprocal plot of a number of these measurements (Figure 4A′) indicated similar V_{max} values (intercept with the *y*-axis) for both actins but different intercepts with the *x*-axis, suggesting lower affinity of S1A1 to the polymerized dimer resulting in K_M values of 1.5×10^{-7} M and 4.5×10^{-7} M for F-actin and polymerized dimer, respectively.

Kim et al. (1998) have shown that isolated actin dimers and oligomers stimulated the myosin ATPase to a considerable extent, albeit less effectively than unmodified F-actin (*12*). Their test system, however, depended on the initiation of S1-induced dimer polymerization after complete hydrolysis of added ATP (*12*). In order to overcome the possible contribution of small amounts of polymeric actin dimer, we decided to test whether polymerization-inhibited dimer was able to stimulate the subfragment 1 ATPase. To this aim, dimer complexed to DNase I, G1, or both proteins was further purified by gel filtration over Sephacryl S300 in G buffer without ATP and added at increasing concentrations to rabbit skeletal muscle myosin subfragment 1 (S1A1). The data of a representative experiment are shown in Figure 4B; they clearly indicate that the dimer in complex with the mentioned actin-binding proteins does not significantly

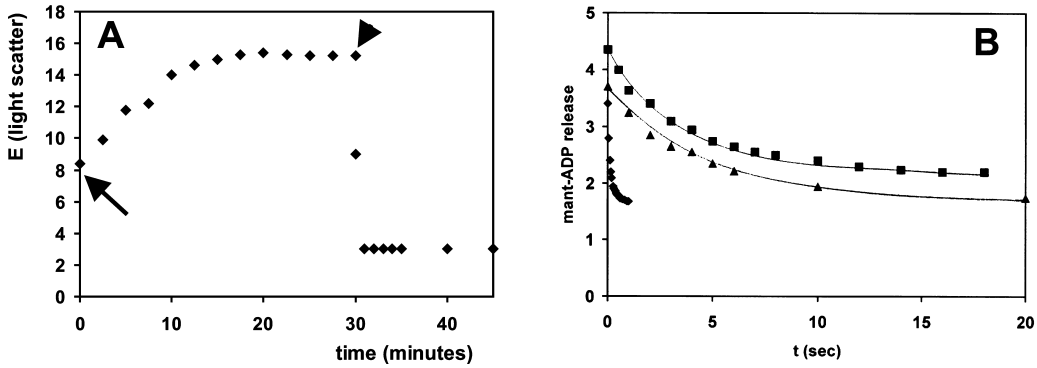

FIGURE 5: Binding of S1A1 to actin dimer is ATP sensitive. (A) G1:AA complex at 1 μM in Hepes buffer (5 mM Hepes-OH, pH 7.4, 0.1 mM $CaCl_2$, 0.5 mM NaN_3, and 0.5 mM DTT) was mixed with 1.27 μM S1A1 at time zero, and the time course of the changes in light scattering was followed with time (abscissa). After 30 min 0.1 mM ATP was added (arrowhead). Note immediate drop in light scattering. (B) Stopped-flow experiments to determine the influence of actin dimer on the rates of mant-ADP release from S1A1. 50 μM S1A1 was preincubated with 0.12 mM mant-ADP for 1 h at room temperature. For the stopped-flow experiments the S1A1 was diluted to 0.5 μM (syringe concentration) and rapidly mixed with an equal volume of 10 μM ATP in Hepes buffer (♦), 1 μM F-actin plus 10 μM ATP (▲), and 20 μM G1:AA plus 10 μM ATP (■). Ordinate gives mant-ADP fluorescence in arbitrary units.

stimulate the S1A1-ATPase as compared to native F-actin. Double-reciprocal plots of these data are given in Figure 4B′ showing a clear difference in the maximal subfragment 1 ATPase rate (V_{max}) between the dimer complexes and native F-actin. Furthermore, different intercepts with the *x*-axis (apparent K_M values) were obtained. For native F-actin and the stable dimer complexes values of about 1.5×10^{-7} M and 5×10^{-7} M were determined, respectively. These data indicate that the dimer complexes bind to S1A1 with a lower affinity, although these K_M values can only be taken as a rough reflection of their binding affinity to S1A1.

Binding of Myosin Subfragment 1 to Dimer Is ATP Sensitive. Although the actin dimer did not significantly stimulate the Mg^{2+}-dependent subfragment 1 ATPase, complex formation between G1:AA and S1A1 was first analyzed by light scattering and subsequently by gel filtration. For these experiments free ATP was removed from the G1:AA complex either by gel filtration over a Sephacryl S300 column or by treatment with the anion-exchange resin (Dowex-1A) for 1 min on ice. Addition of 200 nM S1A1 to 1 μM G1:AA resulted in a slow increase in light scattering that reached a plateau value after about 10 min (Figure 5A). The slow increase in light scattering might have resulted from a slow hydrolysis of residual ATP or polymerization of a small fraction of the actin dimer albeit complexed to G1. Addition of 0.1 mM ATP resulted in an immediate drop of the light scattering (Figure 5A, arrowhead), demonstrating the ATP sensitivity of this interaction, i.e., the rapid dissociation of this complex by ATP.

The Actin Dimer Does Not Significantly Stimulate the Nucleotide Release Step from Subfragment 1. Binding of subfragment 1 to F-actin is a multistep process. During actin-activated ATPase, actin binding sequentially induces the release of inorganic phosphate and ADP concomitant to the generation of contractile force. Since these product-release steps are indicative of a force productive acto-myosin interaction, we tested the effect of actin dimer complexes on the rate of release of fluorescent mant-ADP from S1A1. S1A1 was preincubated with mant-ATP in order to allow its hydrolysis to mant-ADP. The rate of mant-ADP release from subfragment 1 was determined using a stopped-flow setup, which allowed rapid mixing with buffer supplemented with either 5 μM ATP, F-actin plus 5 μM ATP, or actin dimer complexes at increasing concentrations plus 5 μM ATP. Rapid mixing of 0.25 μM S1A1 containing mant-ADP with 5 μM ATP gave a decrease of the mant-ADP fluorescence with a rate constant of 0.09 s^{-1} (Figure 5B). Mixing with 0.5 μM native F-actin plus 0.5 μM ATP resulted in an about 10-fold increase in the rate of mant-ADP release (k_{obs} = 0.95 s^{-1}; Figure 5B). In contrast, rapid mixing with up to 20 μM G1:AA (or 25 μM G1:AA:DNase I, not shown) resulted in a mant-ADP release rate of 0.14 s^{-1}, i.e., an increase of only about 1.6-fold (Figure 5B). The inability of G1:AA to significantly stimulate the rate of ADP release from subfragment 1 may partly explain the lack of S1-ATPase stimulation by the actin dimer complexes. In the actin-activated myosin ATPase reaction, both ADP and phosphate release from the myosin·ADP·P_i complex are accelerated in comparison with the situation without actin, and although phosphate release was not monitored specifically here, we conclude that it is highly likely that actin dimers also have no influence on this step.

Gel Filtration Provides Evidence for Complex Formation between G1:AA and S1A1. We further tested complex formation between G1:AA and S1A1 by gel filtration. First, equimolar G1:AA was gel filtered over Sephacryl S300 in order to remove free ATP. A typical elution profile with an SDS−PAGE analysis of the collected fractions is given in Figure 6A. After concentration of the G1:AA-containing peak fractions with centricon30 an equimolar amount of subfragment 1 was added, incubated for 1 h, and thereafter subjected to gel filtration over Sephacryl S300 in the absence of ATP. The eluted fractions were analyzed by SDS−PAGE (Figure 6B,C). Furthermore, the protein-containing fractions were subjected to immunoblotting using anti-actin and anti-subfragment 1 antibodies (Figure 6D). G1:AA and S1A1 eluted simultaneously at a position corresponding to a higher molecular mass than the individual components, suggesting complex formation.

Determination of the Dissociation Constant of the Dimer: Subfragment 1 Complex. We used fast mixing procedures to analyze the strength of the interaction of cross-linked actin dimer complexed to G1 (G1:AA) with myosin subfragment 1. First we determined the rate constants of association and dissociation of S1A1 to F-actin that was copolymerized with 50% pyrene-actin (F-pyr-actin) and stabilized by phalloidin

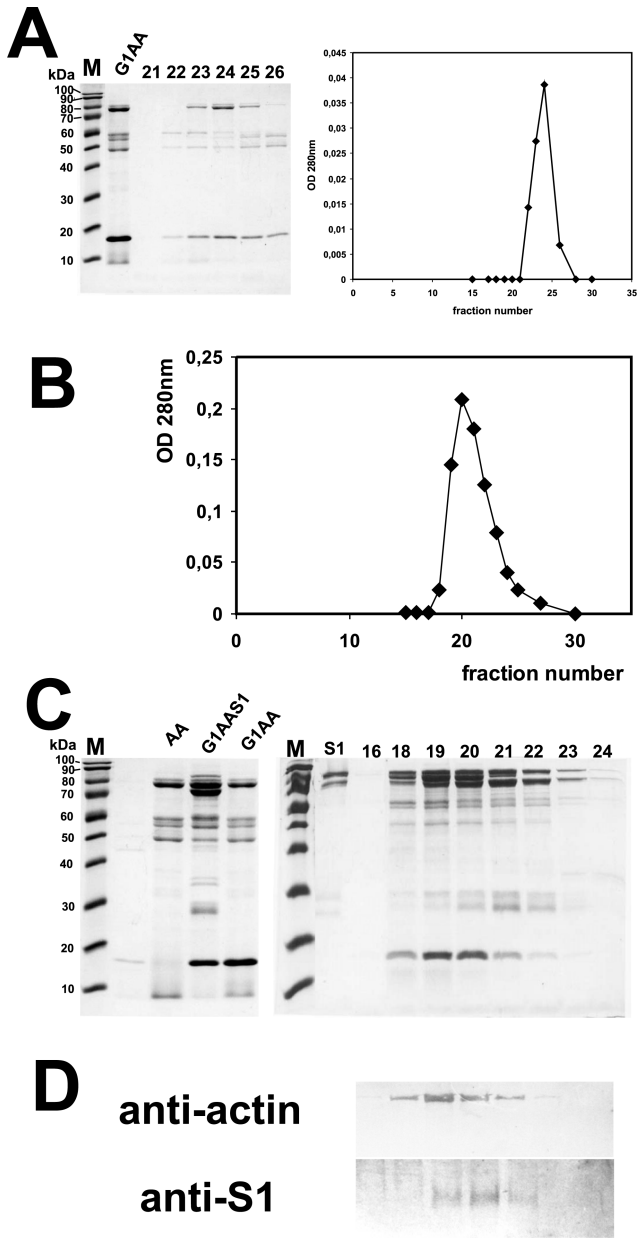

FIGURE 6: Complex formation of G1:AA with S1A1 as determined by gel filtration. (A) Elution profile of gel filtration of G1:AA over Sephacryl S200 (fraction size 1.9 mL) and SDS−PAGE analysis of the peak fractions on a 15% polyacrylamide gel. (B) Elution profile of purified G1:AA complex plus equimolar S1A1 over Sephacryl S200 (fraction size 1.9 mL). (C) gives SDS−PAGE analysis of the samples before gel filtration as indicated over the lanes and fractions collected (fraction numbers are indicated on top of the lanes). (D) gives immunoblots of the collected fractions using anti-actin and anti-myosin subfragment 1 antibodies as detailed in text.

at a 1:0.5 molar ratio. Binding of S1A1 to F-pyr-actin induces a fluorescence decrease. By mixing 0.25 μM S1A1 with 0.25 μM F-pyr-actin the rate constant of S1A1 binding to F-pyr-actin (k_{assoc}) was determined to be 2×10^6 M^{-1} s^{-1}, and by mixing 0.25 μM S1A1-decorated F-pyr-actin with 2.5 μM unlabeled F-actin the rate constant dissociation of S1A1 from F-pyr-actin (k_{dissoc}) was found to be 0.06 s^{-1} giving a dissociation constant of 3×10^{-8} M.

Next, we determined the rates of displacement of 0.25 μM S1A1 bound to equimolar G1:AA after rapid mixing with increasing concentrations of F-pyr-actin (1, 2, and 4 μM).

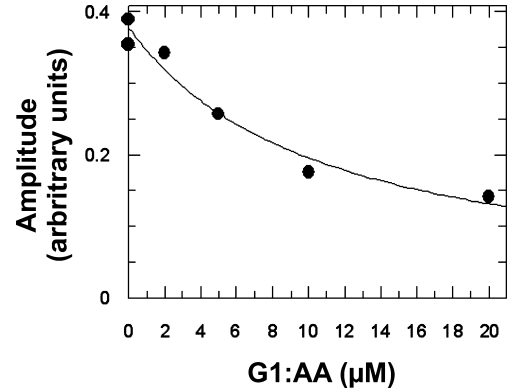

FIGURE 7: Effect of actin dimer complexed to G1 (G1:AA) on the amplitude of the signal change seen on the interaction of F-pyrene-actin with subfragment 1 (S1) in the stopped-flow apparatus. The experiment was performed as described under Materials and Methods using constant concentrations of 0.25 μM F-pyrene-actin and S1. One syringe contained a mixture of F-pyrene-actin and increasing G1:AA, the other S1. Evaluation as described in the Results section leads to a K_d value of 2.4 μM for the S1:AA complex.

The presence of actin dimers had little effect on the result, suggesting that under these concentration conditions there is negligible complex formation, so that the affinity of the complex (using its K_d value as a measure of affinity) is in the μM range or above.

In a final series of experiments, we mixed S1A1 against F-pyr-actin to which increasing concentrations of G1:AA had been added. We observed a decrease in the rate and amplitude of the pyrene fluorescence change caused by competitive binding of S1A1 to the added G1:AA (Figure 7). The exact interpretation of this curve is complicated by the fact that individual rate constants for the association and dissociation of actin dimers form S1A1 are not known, but we can estimate the overall affinity based on the following considerations. Fitting a hyperbolic curve to the amplitude data leads to an apparent K_d value for the actin dimer of 10 μM. This is in competition with a free F-actin concentration of 50% of the total concentration of F-actin used (0.25 μM). Thus, at a concentration of actin dimer of 10 μM it competes on an equal footing with 0.125 μM F-actin, suggesting an 80-fold difference in affinities. Since the K_d value for the S1A1:F-actin complex was shown to be 3×10^{-8} M under the conditions used (see above), this suggests that the K_d value for the G1:AA complex is ca. 2.4×10^{-6} M.

DISCUSSION

The data presented show that the actin dimer chemically cross-linked by ANP (*N*-(4-azido-2-nitrophenyl)) can be purified by gel filtration. This reagent links Gln-41 to Cys-374 of the adjacent monomer along the long-pitch helix of F-actin. We demonstrate that the actin dimer can interact with DNase I and gelsolin segment 1 (G1) and that complexation to these actin-binding proteins inhibits its ability to polymerize. Polymerization of isolated uncomplexed dimer is initiated by increasing the divalent ($MgCl_2$) or monovalent (KCl) cation concentration and also by myosin subfragment 1. In contrast to previous reports (*12*), we observed that the rate and extent of salt-induced polymerization of purified dimer were decreased by about 50% in comparison to unmodified G-actin.

Our data demonstrate that subfragment1 was able to bind to the actin dimer, when complexed to either DNase I or G1 in order to render it unpolymerizable, albeit with a lower affinity than to native F-actin. Binding of subfragment 1 to G1:AA was also demonstrated by gel filtration. Using fast mixing techniques and F-actin containing 50% of pyrene-labeled subunits, it was shown that actin dimer binds with ca. 80-fold lower affinity than F-actin to S1 ($K_d = 2.4 \times 10^{-6}$ for actin dimer, 3×10^{-8} M for F-actin).

Current models based on chemical cross-linking (*27*) and image reconstruction of S1-decorated F-actin (*6, 7, 28*) suggest that the binding area of subfragment 1 on F-actin comprises two adjacent actin monomers along the long-pitch helix. We therefore hoped that the isolated actin dimer would fully mimic the properties of F-actin. However, it was found that the dimer did not stimulate the Mg^{2+}-dependent S1-ATPase and only slightly the rate of mant-ADP release from subfragment 1. In this respect the dimer behaved similarly to G-actin (*18*), which binds S1A1 with lower affinity and is also unable to significantly stimulate its ATPase activity, but was found to be able to stimulate mant-ADP release from S1 (*18*).

During the cross-bridge cycle of actively contracting muscle, the myosin heads interact with actin in a complex fashion that has been thoroughly analyzed by kinetic procedures (see ref *29*). The cross-bridge cycle and in particular the bound state can be divided into several steps that are linked to successive product release steps from the myosin head after ATP hydrolysis. Therefore, the low ability of actin dimer to stimulate mant-ADP release from S1A1 might be taken as evidence that the dimer-bound subfragment 1 was either arrested in an initial binding step, mediated by weak ionic interactions (*9, 30*), or rapidly dissociated and therefore unable to proceed to further states during the attachment phase necessary for the effective stimulation the product release steps from S1. This could be due to an incorrect orientation of the two actin subunits within the dimer or a persistence of the G conformation. It is conceivable that the correct F conformation will only be adopted in the presence of subunits of the second strand. Alternatively, the cross-linker might have led to a restriction of the conformational and/or rotational mobility of the subunits, thus hindering the possibility to perform isomerization steps.

It may also be argued that complexation of the actin dimer with either DNase I or/and G1 might have changed the relative monomer orientation or induced a G conformation thereby impairing binding of subfragment 1. Indeed, the crystal structure of the complex of three G1 molecules with an actin trimer cross-linked along the genetic helix demonstrated that G1 was able to intercalate between adjacent actin monomers and to increase the subunit distance from 5.5 to 7.58 nm (*31*). We regard this possibility, however, as unlikely for the long-pitch dimer, because it would necessitate stretching of the cross-linker itself (that has a length of 12 nm) and because native gel electrophoresis indicated only one G1 was bound to the actin dimer. However, binding of G1 to the dimer increased its apparent affinity to DNase I. This effect could be attributed to an alteration of the orientation or conformation of subdomain 2 of the subunit bound to G1. Intramolecular allosteric effects of the actin conformation, in particular to its subdomain 2, have been previously described (*32*). Such conformational alteration after G1 binding might also occur during the F-actin severing action by intact gelsolin when the G1 segment first intercalates between adjacent actin subunits of the long-pitch strand (*3*).

The observation that stimulation of the S1-ATPase by native F-actin was almost double of that of filaments generated from cross-linked actin dimer (in the absence of an actin-binding protein) suggests that only the unmodified actin−actin contacts contributed to the ATPase stimulation. Therefore, it is possible that the cross-linking reaction itself introduced structural modifications incompatible with high-affinity S1:F-actin interaction. Indeed, it has been reported that F-actin containing increased amounts of cross-linked dimer exhibited a progressive reduction of the speed of F-actin movement in the in vitro motility assay (*14, 15*). Alternatively, the binding of G1 may have induced a G conformation of at least the bound subunit as demonstrated by the increased affinity to DNase I and thereby reduced its ability to stimulate the myosin subfragment 1 ATPase.

Negative staining and image reconstruction of polymerized cross-linked actin did not give evidence for significant changes in its morphology as compared to native F-actin (*12, 14*). However, the recent crystallographic structure analysis of actin dimer additionally chemically modified by tetramethylrhodamine maleimide (TRM) at the free Cys-374 in order to inhibit its polymerization indicated a high structural disorder of subdomain 2 and a loss of the helical rotation present in F-actin (*13*). The higher disorder of subdomain 2 might have been induced by the TMR modification and might explain our observation that only one DNase I molecule is inhibited by dimer on its own, even though both actins of the cross-linked dimer are able to bind DNase I. It seems most likely that DNase I inhibition is not effected by the actin subunit, whose DNase I loop (subdomain 2) is cross-linked via Gln-41 to Cys-374 of subdomain 1 of the upper monomer. Analysis of the dimer crystal did not allow the identification of the cross-linker, since the asymmetric unit contained only one actin molecule (*13*). Therefore, it was not possible to correlate the observed disorder of subdomain 2 to the cross-linking reaction.

As suggested above, the 50% reduction of S1A1-ATPase stimulation by polymerized dimer might arise from the unmodified, i.e., non-cross-linked actin−actin long-pitch interfaces that will not be distorted or restrained in their flexibility by the cross-linker. The location of the disordered subdomain 2 in the contact area of the two actins and their straight orientation might both impair full functional binding of subfragment 1. Together with the fact that purified cross-linked actin dimer hardly stimulates the nucleotide release and the S1-ATPase, this result might be taken as a further indication for the necessity of rotational and/or conformational dynamic changes of the actin−actin interface for full functional interaction with myosin heads (*33*). Indeed, a recent EPR study of ANP-cross-linked F-actin demonstrated a large decrease in rotational mobility of a spin probe attached to the unmodified Cys-374 (*34*). The same authors demonstrated that addition of heavy meromyosin loaded with ADP and inorganic phosphate (HMM-ADP-P_i) did not result in EPR signals typical for the transition from the weakly to strongly bound state (*33*) necessary for the actin-stimulated P_i and subsequently ADP release from myosin heads.

Our data demonstrating that the cross-linked dimer does not fully functionally interact with myosin subfragment 1 do not preclude the current model that the long-pitch actin−actin contact area forms its primary binding site. The zero-length cross-linker ANP appears to impair rotational motions of adjacent monomers relative to each other, or it may induce conformational changes of single monomers and thereby prevent fully functional actin−myosin interactions. Therefore, our results can be taken as evidence for a more active participation of actin via myosin-induced conformational changes during the force generating cross-bridge cycle. Alternatively, the functionally optimal binding area for myosin heads might include additional actin molecules from the opposing strand, or more than two actin monomers along the same long-pitch strand have to be contacted by a myosin head in order to accomplish ATP hydrolysis during the execution of an effective cross-bridge cycle (*35*).

ACKNOWLEDGMENT

It is pleasure to thank Mrs. Ulricke Ritenberg for expert technical assistance and Dr. Dietmar Manstein (Hannover, Germany) for helpful comments on the manuscript.

REFERENCES

1. Straub, F. B. (1942) Actin, in *Studies from the Institute of Medical Biochemistry*, Vol. 3, pp 23−37, University of Szeged, Szeged, Hungary.
2. Kabsch, W., Mannherz, H. G., Suck, D., Pai, E., and Holmes, K. C. (1990) The atomic structure of actin:DNase I complex. *Nature 347*, 37–44.
3. McLaughlin, P. J., Gooch, J., Mannherz, H. G., and Weeds, A. G. (1993) Atomic structure of gelsolin segment 1 in complex with actin and the mechanism of filament severing. *Nature 364*, 685–692.
4. Schutt, C. E., Myslik, J. C., Rozycki, M. D., Goonesekere, N. C., and Lindberg, U. (1993) The structure of crystalline profilin-beta-actin. *Nature 365*, 810–816.
5. Otterbein, L. R., Cosio, C., Graceffa, P., and Dominguez, R. (2002) Crystal structures of the vitamin D-binding protein and its complex with actin: structural basis of the actin-scavenger system. *Proc. Natl. Acad. Sci. U.S.A. 99*, 8003–8008.
6. Rayment, I., Holden, H. M., Whittaker, M., Yohn, C. B., Lorenz, M., Holmes, K. C., and Milligan, R. A. (1993) Structure of the actin-myosin complex and its implications for muscle contraction. *Science 261*, 58–65.
7. Schröder, R. R., Manstein, D. J., Jahn, W., Holden, H., Rayment, I., Holmes, K. C., and Spudich, J. A. (1993) Three-dimensional atomic model of F-actin decorated with Dictyostelium myosin S1. *Nature 364*, 171–174.
8. Holmes, K. C., Popp, D., Gebhard, W., and Kabsch, W. (1990) Atomic model of the actin filament. *Nature 347*, 44–49.
9. Holmes, K. C., Tirion, M., Popp, D., Lorenz, M., Kabsch, W., and Milligan, R. A. (1993) A comparison of the atomic model of F-actin with cryo-electron micrographs of actin and decorated actin. *Adv. Exp. Med. Biol. 332*, 15–22.
10. Hegyi, G., Michel, H., Shabanowitz, J., Hunt, D. F., Chatterjie, N., Healy-Louie, G., and Elzinga, M. (1992) Gln-41 is intermolecularly cross-linked to Lys-113 in F-actin by *N*-(4-azidobenzoyl)-putresceine. *Protein Sci. 1*, 132–144.
11. Hegyi, G., Mák, M., Kim, E., Elzinga, M., Muhlrad, A., and Reisler, E. (1998) Intrastrand cross-linked actin between Gln-41 and Cys-374. I. Mapping of sites cross-linked in F-actin by *N*-(4-azido-2-phenyl) putresceine. *Biochemistry 37*, 17784–17792.
12. Kim, E., Phillips, M., Hegyi, G., Muhlrad, A., and Reisler, E. (1998) Intrastrand cross-linked actin between Gln-41 and Cys-374. II. Properties of cross-linked oligomers. *Biochemistry 37*, 17793–17800.
13. Kudryaskov, D. S., Sawaya, M. R., Adisetiyo, H., Norcross, T., Hegyi, G., Reisler, E., and Yeates, T. O. (2005) The crystal structure of a cross-linked actin dimer suggests a detailed molecular interface in F-actin. *Proc. Natl. Acad. Sci. U.S.A. 102*, 13105–13110.
14. Kim, E., Bobkova, E., Miller, C. J., Orlova, A., Hegyi, G., Egelman, E. H., Muhlrad, A., and Reisler, E. (1998) : Intrastrand cross-linked actin between Gln-41 and Cys-374. III. Inhibition of motion and force generation with myosin. *Biochemistry 37*, 17801–17809.
15. Kim, E., Bobkova, E., Hegyi, G., Muhlrad, A., and Reisler, E. (2002) Actin cross-linking and inhibition of the actomyosin motor. *Biochemistry 41*, 86–93.
16. Hiratsuka, T. (1985) Photosensitized direct cross-linking of fluorescent analogs of ATP to the adenine recognition domain in myosin ATPase. *J. Biochem. (Tokyo) 97*, 71–78.
17. Mannherz, H. G., Gonsior, S., Wu, X., Polzar, B., Pope, B., Wartosch, L., and Weeds, A. G. (2006) Dual effects of staurosporine on A431 and NRK cells: immediate ADF/cofilin activation causes microfilament disassembly and increased lamellipodial activity followed by cell death. *Eur. J. Cell Biol. 85*, 785–802.
18. Ballweber, E., Kiessling, P., Manstein, D., and Mannherz, H. G. (2003) The interaction of myosin subfragment 1 with forms of monomeric actin. *Biochemistry 42*, 3060–3069.
19. Mannherz, H. G., Goody, R. S., Konrad, M., and Nowak, E. (1980) The interaction of bovine pancreatic deoxyribonuclease I and skeletal muscle actin. *Eur. J. Biochem. 104*, 367–379.
20. Way, M., Gooch, J., Pope, B., and Weeds, A. G. (1989) Expression of human plasma gelsolin in Escherichia coli and dissection of the actin binding sites by segmental deletion mutagenesis. *J. Cell Biol. 109*, 593–605.
21. Weeds, A. G., and Taylor, R. S. (1975) Separation of subfragment-1 isoenzymes from rabbit skeletal muscle myosin. *Nature 257*, 54–56.
22. Kouyama, T., and Mihashi, K. (1981) Fluorimetry study of N-(1-pyrenyl)iodoacetamide-labelled F-actin. Local structural change of actin protomer both on polymerization and on binding of heavy meromyosin. *Eur. J. Biochem. 114*, 33–38.
23. Bradford, M. M. (1976) A rapid and sensitive method for the quantitation of microgram quantities of protein utilizing the principle of protein-dye binding. *Anal. Biochem. 72*, 248–254.
24. Laemmli, U. K. (1970) Cleavage of structural proteins during the assembly of the head of bacteriophage T4. *Nature 227*, 680–685.
25. Ballweber, E., Galla, M., Aktories, K., Yeoh, S., Weeds, A. G., and Mannherz, H. G. (2001) Interaction of ADP-ribosylated actin with actin binding proteins. *FEBS Lett. 508*, 131–135.
26. Polzar, B., Nowak, E., Goody, R. S., and Mannherz, H. G. (1989) The complex of actin and deoxyribonuclease I as a model system to study nucleotide-, cation-, and cytochalasin D-interactions with monomeric actin. *Eur. J. Biochem. 182*, 267–275.
27. Mornet, D., Bertrand, R., Pantel, P., Audemard, E., and Kassab, R. (1981) Structure of the actin-myosin interface. *Nature 292*, 301–306.
28. Amos, L. A., Huxley, H. E., Holmes, K. C., Goody, R. S., and Taylor, K. A. (1982) Structural evidence that myosin heads may interact with two sites on F-actin. *Nature 299*, 467–469.
29. Geeves, M. A., and Holmes, K. C. (1999) Structural mechanism of muscle contraction. *Annu. Rev. Biochem. 68*, 687–728.
30. Furch, M., Remmel, B., Geeves, M. A., and Manstein, D. (2000) Stabilization of the actomyosin complex by negative charges on myosin. *Biochemistry 39*, 11602–11608.
31. Dawson, J. F., Sablin, E. P., Spudich, J. A., and Fletterick, R. J. (2003) Structure of an F-actin trimer disrupted by gelsolin and implications for the mechanism of severing. *J. Biol. Chem. 278*, 1229–1238.
32. Khaitlina, S. Y., and Strzelecka-Golaszewska, H. (2002) Role of the DNase-I-binding loop in dynamic properties of actin filament. *Biophys. J. 82*, 321–334.
33. Kozuka, J., Yokota, H., Arai, Y., Ishii, Y., and Yanagida, T. (2006) Dynamic polymorphism of single actin molecules in the actin filament. *Nat. Chem. Biol. 2*, 83–86.
34. Hegyi, G., and Belágyi, J. (2006) Intermonomer cross-linking of F-actin alters the dynamics of its interaction with H-meromyosin in the weak binding state. *FEBS J. 273*, 1896–1905.
35. Kitamura, K., Tokunaga, M., Iwane, A. H., and Yanagida, T. (1999) A single myosin head moves along an actin filament with regular steps of 5.3 nanometres. *Nature 397*, 129–134.

BI800410Z